# A Data Acquisition and Processing System for 3-D Position Sensitive CZT Gamma-ray Spectrometers

W. Li[1], Z. He, G.F. Knoll, D.K. Wehe, J.E. Berry
Department of Nuclear Engineering and Radiological Sciences,
University of Michigan, Ann Arbor, MI 48109, U.S.A.

## *Abstract*

A PC-based data acquisition and processing system has been developed for two 3-D position-sensitive CZT $\gamma$ ray detectors. For each 3-D CZT detector, an integrated readout chip (VA1) is used to read out the signals from the $11\times11$ anode pixels. Two independent preamplifiers are used to read out the signals from the cathode and the grid electrodes that are used as trigger signals for low and high energy incident $\gamma$ rays, respectively. A PC-based DAQ board samples the amplitudes of the signals from the anode pixels and the cathode. The software collects and processes the energy spectra from the sampling data. The typical equivalent electronic noise of this system is measured to be 6 keV and 7 keV for the two 3-D CZT detectors, and the dynamic range of the system is up to 1 MeV. Spectra from 60, 122 and 662 keV $\gamma$ rays have been successfully measured using the two 3-D CZT detectors.

## I. Introduction

The two 3-D position sensitive CZT gamma-ray detectors are the first fully functional solid state detectors which provide the 3-D location of gamma-ray interactions inside the detector volume[1]. This unique characteristic makes these 3-D CZT detectors attractive in imaging applications as well as for high energy resolution gamma spectroscopy at room temperature. The 3-D position sensitive CZT detector is fabricated with a pixellated anode and a single cathode. For each incident $\gamma$ ray interaction event, the amplitude of the signals from the anode pixels and cathode need to be read out and combined together to determine the amount and 3-D position of the energy deposition (For single-site interaction, the interaction location in the lateral dimension is determined by the position of the anode pixel producing the signal, and the interaction depth is given by the ratio of the signals from the cathode and the anode pixel.). This paper describes the development of a PC-based data acquisition and processing system for our two 3-D CZT detectors, each detector having an $11\times11$ pixellated anode.

An integrated multiple-channel readout chip is used to read out the signals from $11\times11$ anode pixels. Each of the two 3-D CZT detectors is a 1 $cm^3$ cubic crystal. The energy range of interest is from a few keV to $\sim$1 MeV. Therefore, the equivalent dynamic range of the readout chip must be at least 1 MeV(which precludes some candidate chips). In addition, the expected energy resolution implies the equivalent electronic noise of the system should be no more than a few keV. The ASIC VA1 chip from IDE AS[2] meets the above requirements and was adopted as the front end of the 3-D CZT detectors. Each VA1 chip has 128 independent signal readout channels, and its equivalent dynamic range and electronic noise are $\sim$1 MeV and 0.8 keV + 0.033 keV/pF rms respectively for CZT[2]. Two separate charge-sensitive preamplifiers (A250) from AMPTEK[3] are used to read out the signals from the cathode and grid electrode. These two signals are necessary in monitoring the working condition of the detector, and in providing the system trigger signal for the triggerless VA1 chip. The AT-MIO-16E-1 DAQ board from National Instruments is used as the A/D converter. The additional D/A converter, timers and DIO lines on this board are used to generate analog and digital signals for system testing and control.

The software of the system evaluates the performance of the VA1 chip, and collects and processes energy spectra. For evaluating the VA1 chip, the baseline and the response to a testing signal are automatically measured for all VA1 channels over a short time. This function is very useful to quickly check the working condition of VA1 chip, especially after the biases applied to the detector are changed. In spectra collection and processing, voxel-based $\gamma$ spectra underneath each anode pixel have been collected by using the depth sensing technology[4]. A subsequent 3-D nonuniformity correction yields an improved energy resolution throughout the detector.

This paper also addresses three issues which are closely related to the performance of this data acquisition system: electronic noise from the DC-coupling between the detector and the VA1 chip, triggering signal selection, and gain drift in the system.

## II. System Description

The VA1 chip has 128 independent readout channels. Each channel is identical and includes a preamp, a shaper and a sample/hold circuit. For an event from the detector, the outputs of the 128 channels are read out serially through a multiplexer built on the chip. This working mode of parallel processing and series readout simplifies the communication with the following circuitry, but at the expense of a long dead time from serially reading each channel in the VA1 chip. Sparse readout capability would increase this throughput rate, but is unavailable on the VA1 chip. The event processing rate of our current DAQ system is $\sim$1 K/sec.

The block diagram of our current DAQ system is shown in Fig. 1. For each 3-D CZT detector a VA1-based hybrid/repeater module from IDE AS is used to read out the signals from $11\times11$ anode pixels. The hybrid board provides physical support and fanout signal connections to the VA1 chip, and the repeater card interfaces the VA1 chip to the following DAQ

[1]E-mail: wenli@engin.umich.edu

0018-9499/99$10.00 

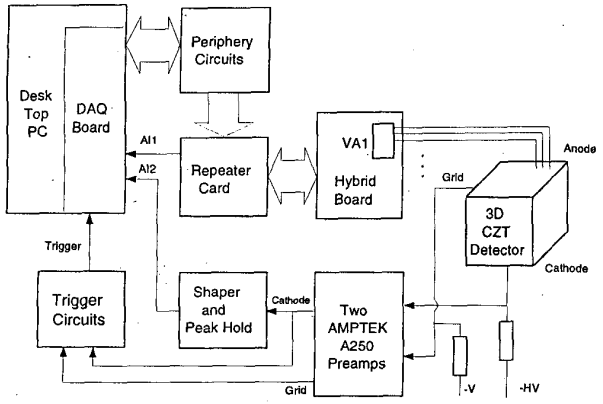


Figure 1: System block diagram.

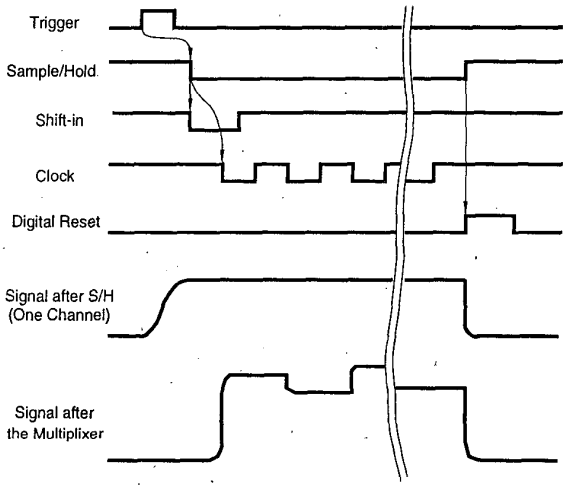


Figure 2: The control signals of the DAQ system and corresponding output from VA1 chip.

circuits. The periphery circuit performs the level shift from TTL to differential TTL for the digital control signals sent to the repeater card, and also generates the clock signal which synchronizes the A/D conversion and VA1 channel switching. The control signals of this system are shown in Fig. 2. For each interaction event in the detector, the system trigger signal is generated by the trigger circuits from either the cathode signal or grid signal. Initiated by the trigger signal, the DAQ board and periphery circuits generate the four digital control signals for VA1 chip: Sample/Hold, Shift-in, Clock and Digital-reset. The falling edge of Sample/Hold signal holds the signal of VA1 readout channel at the peak (if the timing is correct), then the first clock pulse works with the valid (low) Shift-in signal to start the channel switching. Each falling edge of the clock signal switches the output of VA1 chip to the next channel and starts the corresponding A/D conversion. After the 128th clock pulse, all of the VA1 channels have been read out, the Sample/Hold signal returns to high and initiates the Digital-reset signal to reset the VA1 chip.

## A. *Sample/Hold Signal Timing*

In our system, the Sample/Hold signal is generated by a programmable timer on the DAQ board. Triggered by a system trigger signal, the timer outputs the Sample/Hold signal after certain delay. The length of delay and the pulse width are preset by software. The delay is set according to the shaping time of the shapers on VA1 chip to make the beginning of the Sample/Hold signal coincide with the peak of the signal from each shaper. The pulse width is set to be long enough to cover the channel switching and A/D conversion time. Since the timer uses the 20 MHz clock on the DAQ board, the maximum time walk on the Sample/Hold signal due to the timer itself is 50 ns. The relative error in amplitude sampling induced by this time interval is less than 0.3% and so is negligible when the shaping time of VA1 chip is larger than 1 $\mu$s.

## B. *System Trigger Signal*

The system trigger signal has to be generated from the cathode or the grid signal since it is not available from the VA1 chip. Because the Sample/Hold signal is initiated by the system trigger signal, the trigger signal needs to have a constant timing relation to the pixel signal to guarantee accurate sampling of peak amplitude. The signals from the cathode and the anode pixels have a depth-dependent timing relation, and variations arise from the different electron drift times from the interaction location to the anode. Thus, the cathode signal can not be used to generate the trigger signal when interactions may occur at any depth. Instead the transient signal from the anode grid is used to generate the trigger signal. Fig. 3 shows the signal waveforms for two single-pixel events from 662 keV photons. The waveforms of the cathode and the grid signals are recorded from the outputs of the preamplifiers. The waveform of the pixel signal is taken after the shaper on the VA1 chip. The interaction depth of event 1 is near the anode surface, and the interaction depth of event 2 is near the cathode surface. From Fig. 3 we can see clearly the sharply falling edges on the grid signals which correspond to the time when electrons are collected by the anode pixel. These sharp falling edge coincide with the starting times of the pixel signals. In the trigger circuits, a differentiator is used with a threshold circuit to pick out the falling edge and generate the system trigger signal. Because the grid signal is transient, the signal-to-noise ratio is poor. As a result, the energy threshold of this triggering mode is kept larger than 100 keV, which precludes detecting low energy $\gamma$ rays in this mode.

Fortunately, for the detection of low energy $\gamma$ rays, most of the interactions should occur near the surface of the detector. By irradiating from the cathode side, the cathode signal can generate the system trigger signal. In this case the cathode signal has the best signal-to-noise ratio and nearly constant timing relation to the pixel signal. The energy threshold can be under 10 keV.

For multiple-pixel events arising from multiple interactions, the signals may not be sampled accurately if the multiple interactions occur at different depths. To demonstrate this, Fig. 4 shows the waveform of the grid signal for a two-pixel

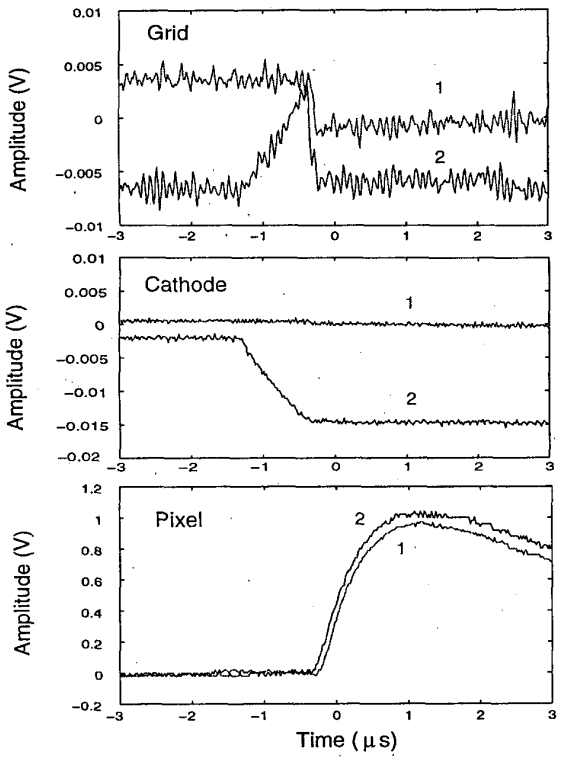


Figure 3: Signal waveforms from two events in 3-D CZT detector. Event 1: near anode surface. Event 2: near cathode surface.

event from a 662 keV $\gamma$ ray. The two falling edges indicate that two interactions occurred at different depths. In grid triggering mode the system trigger signal will be initiated by the first falling edge, so the pixel signal corresponding to the second falling edge will be sampled earlier than the peak. Theoretically this sampling error can be corrected if we know the time interval $\Delta$t between the two falling edges. Furthermore, with $\Delta$t we can also determine the locations of the two relevant interactions and apply accurate nonuniformity corrections for the two-pixel event.

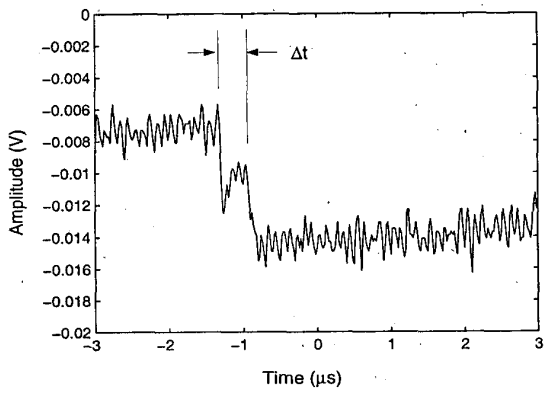


Figure 4: Waveform of grid signal in a multiple-pixel event

To test our ability to distinguish the two events, we developed a trigger circuit using a differentiator with a small time constant, so that after the threshold circuit, the output was two narrow trigger pulses corresponding to the two falling edges. The two trigger pulses were sent to a TAC to determine the $\Delta$t. Using a cathode bias of -1000 V and a maximum $\Delta$t of 1 $\mu$s, this method can provide the $\Delta$t for two-pixel events with $\Delta$t larger than $\sim$0.4 $\mu$s. Unfortunately, the cathode bias has to be increased to about -2000 V to achieve the best energy resolution from single-pixel events. In this case the maximum value of $\Delta$t is reduced to 0.5 $\mu$s, and it is difficult to accurately measure $\Delta$t with our circuitry for most two-pixel events. This problem is being addressed currently.

## C. Electronic Noise

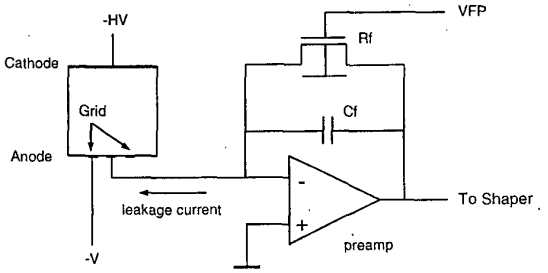


Figure 5: The input of the preamp of VA1 chip.

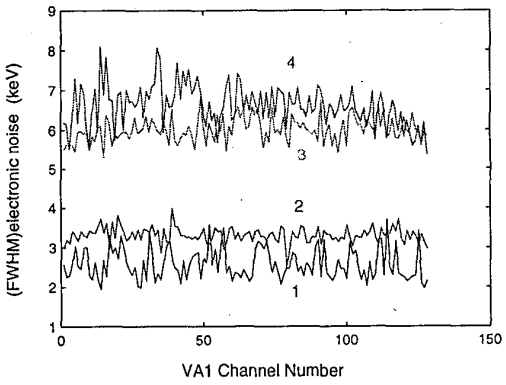


Figure 6: The electronic noise for each VA1 channel.

The electronic noise of this system is due mainly to the preamplifier on the VA1 chip. A schematic plot of a preamplifier and its connection to the detector is shown in Fig. 5. An FET is used as a feedback resistor to perform the discharge of the preamplifier. The equivalent resistance value Rf of the FET can be adjusted by shifting the FET bias VFP. In order to minimize the induced noise, Rf is usually kept as high as possible while allowing the preamplifier to discharge properly. In our two 3-D CZT detectors, the anode pixels are directly wirebonded to the input pads of VA1 channels to form the DC coupling. Without any applied detector bias, the equivalent electronic noise of the VA1 chip in the two 3-D CZT detectors were measured before and after the wirebonding. Similar results were acquired for both detectors. Fig. 6 shows the results for detector #1 before (case 1) and after (case 2) the wirebonding in FWHM of equivalent energy. The equivalent electronic noise in both cases is around 3 keV and approach the

manufacturer's performance claims. The slight increase in case 2 is attributable to the increased capacitance from wirebonding.

After the detector biases are applied, leakage current flows through the pixels and through the feedback FETs of the preamps because of the DC-coupling. Under normal detector biases the leakage current flowing through a pixel is around a few nA, which could saturate the preamp if the feedback FET works in its normal condition. To compensate, VFP needs to be adjusted so the preamp can tolerate larger leakage current. Unfortunately, the equivalent electronic noise then increases due to the reduced value of Rf. For detector #1, Fig. 6 shows the results after VFP was adjusted for operation with a cathode bias of -2400 V and grid bias of -50 V. The electronic noise of the VA1 chip was measured with (case 4) and without (case 3) the detector biases. The results clearly show the increased noise associated with reducing Rf.[2] The electronic noise of the VA1 chip (around 7 keV) should be significantly improved by introducing AC or AC equivalent coupling between the VA1 chip and the detector.

## D. *Spectrum Stabilization*

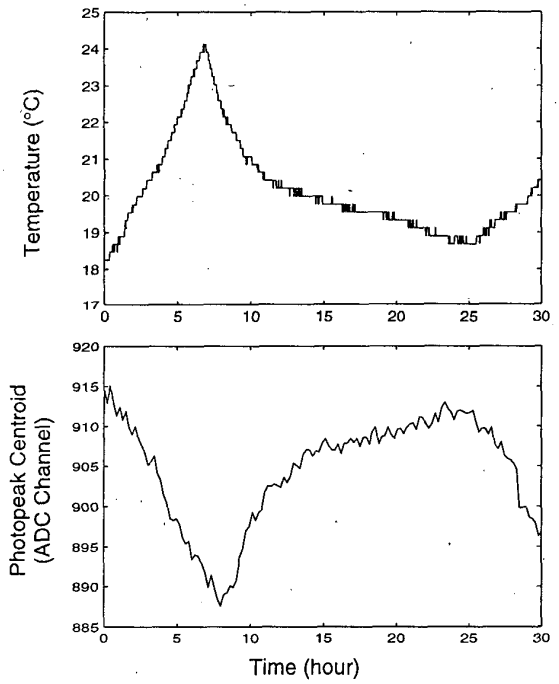


Figure 7: Variation of temperature and drift of photopeak centroid at 662 keV in 30 hours.

In the test of system stability, the drift of the gain of the VA1 chip was observed while the ambient temperature changed. Fig. 7 shows the variation of ambient temperature and the drift of 662 keV photopeak centroid as measured by a 3-D CZT detector over 30 hours. During the experiment the baseline of the VA1 chip was also recorded and no obvious drift was observed, showing that any drift of the photopeak centroid is due to the variation of system gain. The temperature coefficient of the relative gain is around -0.5%/°C and quite uniform for each VA1 channel.

In spectra collected with a 3-D CZT detector, the collection time extends to as long as a few days for adequate statistics in the voxel-based spectra. This is because the low activity of the radiation source and low count rate capability of the serial readout. During this long period, the spectrum stabilization is performed by gain correction software. Only one gain correction coefficient is needed because the temperature coefficients are quite uniform for all VA1 channels. To determine the gain correction coefficient, a prominent photopeak in the spectrum is normally needed as the reference peak. The gain correction coefficient is updated periodically according to the reference photopeak centroid from the spectrum collected in most recent preset time interval. This method works well if a prominent photopeak is available in the energy spectrum being measured. For example, Fig. 8 shows the difference of the $^{137}$Cs spectra simultaneously collected from a voxel of detector #1 with and without spectrum stabilization. During the collection of ~70 hours the ambient temperature varied in the range from 18 °C to 24 °C. Without a photopeak present in the spectrum, temperature-dependent gain corrections may be investigated as an alternative stabilization method.

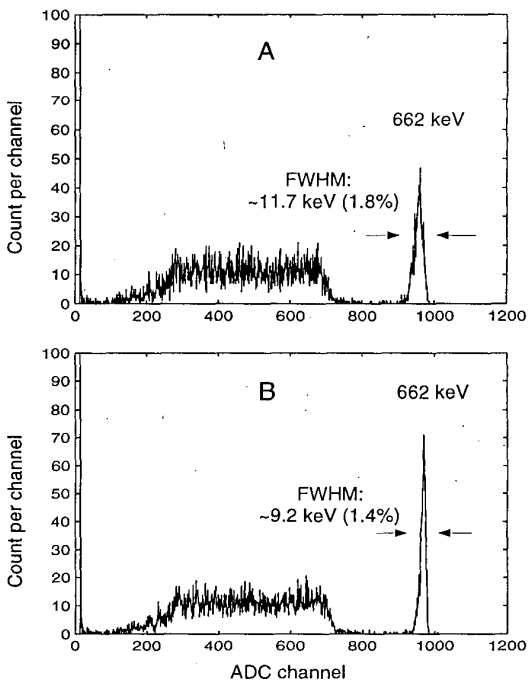


Figure 8: $^{137}$Cs spectrum of single-pixel events from a voxel in detector #1, collected over ~70 hours. A: without stabilization B: with stabilization

[2]For detector #2, a higher leakage current and limit on the VFP adjustment limited the cathode bias to only -1400 V with grid bias of -50 V. The electronic noise of the VA1 chip was still measured to be ~6 keV.

### E. Software

The software for system testing was developed using Labview. In testing mode, the software tells the DAQ board to send a test signal to the VA1 chip and read the response. The amplitude of the test signal is determined by the output of the DAC unit on the DAQ board, which is also controlled by the software. By this means, the software can automatically measure the baseline and the responses to test signals for each of the 128 VA1 channels. The electronic noise and dynamic range of each VA1 channel are available from the measurement results, which is important in monitoring the working condition of the VA1 chip.

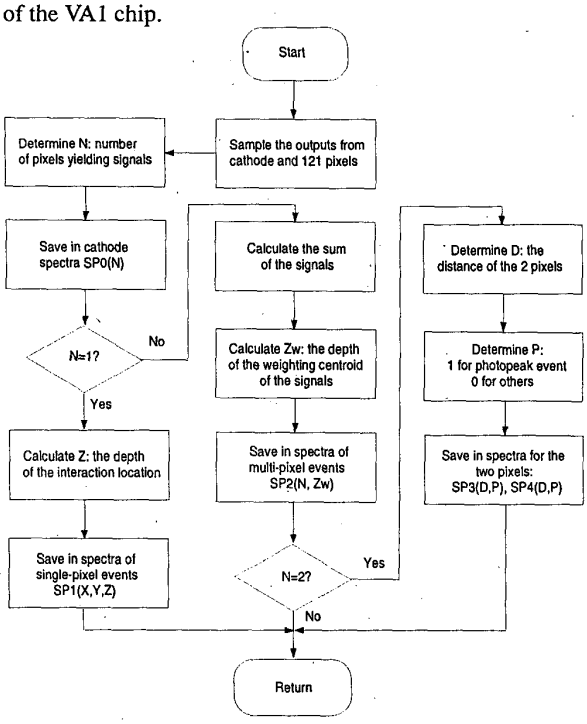


Figure 9: Flow chart of software for recording one interaction event.

The software for spectrum collection and processing is written in C for its fast access to large memory blocks necessary in spectrum storage. The flow chart of the software for recording one interaction event in spectrum collection is shown in Fig. 9. For a single-pixel event, after the amount of energy deposition and the 3-D interaction location are determined, the event is recorded in the corresponding energy spectra in an $11\times11\times20$ voxel-based spectra array. For a multi-pixel event, after the total energy deposition and the depth of the weighted center of interactions are determined, the event is recorded in another spectra array according to the depth of interaction center and the number of pixels yielding signals for the event. For 2-pixel events, more information (including the distance between the two pixels and the energy spectra from each pixel) is also recorded. This information is used in the investigation of the signal sharing between two pixels[5][6].

From the voxel-based energy spectra array of single-pixel events, the 3-D distribution of photopeak count rate, photopeak centroid and energy resolution can be obtained and used in the nonuniformity analysis of detector material. In the application of gamma spectroscopy, the 3-D distribution of the photopeak centroid can be used to register the spectra from all the voxels and yields an overall spectrum from the whole detector with high energy resolution.

## III. Experimental Results

The energy spectra from $^{241}$Am, $^{57}$Co and $^{137}$Cs have been successfully collected from both detectors with this system. The $^{241}$Am and $^{57}$Co spectra are collected with the gamma rays incident from the cathode side, so the cathode signal is used to generate the system trigger signal. As expected, most of the interaction events from $^{241}$Am and $^{57}$Co gamma rays were recorded in spectra corresponding to the voxels near the cathode surface. Fig. 10 shows the $^{241}$Am spectrum of single-pixel events collected from the whole bulk of detector #1 after the voxel-based nonuniformity correction. During the collection the cathode bias was -2000 V and the grid bias is -50 V. The FWHM of 6.8 keV at the 60 keV photopeak is dominated by the electronic noise of the VA1 chip.

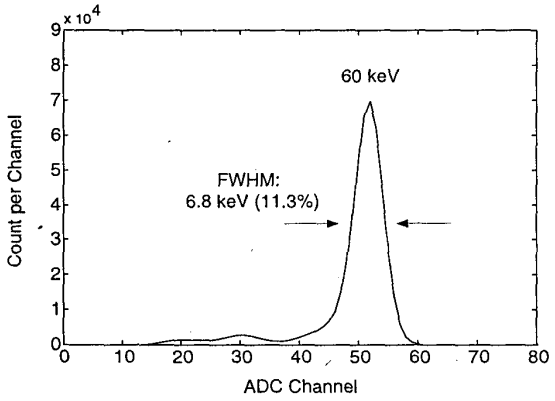


Figure 10: $^{241}$Am spectrum of single-pixel events from the whole bulk of 3-D CZT detector #1.

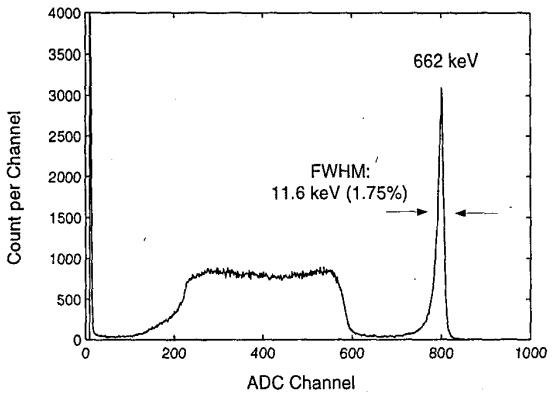


Figure 11: $^{137}$Cs spectrum of single-pixel events from the whole bulk of 3-D CZT detector #1.

The $^{137}$Cs spectra were collected using the grid signal to generate the system trigger signal. In this case the interaction

events are spread throughout the whole volume of the detector, and the energy spectra were collected from the cathode to the anode. Because of the poor signal-to-noise ratio on the grid signal, the energy threshold could not be adjusted below 100 keV. Fig. 11 shows the $^{137}$Cs spectrum of single-pixel events collected from the whole bulk of detector #1 after the voxel-based nonuniformity correction. The FWHM of 11.2 keV at 662 keV indicates significant contributions to the resolution other than the electronic noise from VA1 chip. These include the contributions from the detector[7][8] and the data acquisition system (e.g., the temperature effects on VA1 chip gains and time walk on the Sample/Hold signal).

## IV. Summary and Prospects

We have developed a data acquisition and processing system for the application of 3-D position sensitive CZT detectors in gamma spectroscopy. The equivalent electronic noise of this system is around 6-7 keV for our two 3-D CZT detectors, and is limited by the DC-coupling between the VA1 chip and the detector. In the cathode triggering mode for the measurement of low energy $\gamma$ rays, the energy threshold can be kept below 10 keV and the energy resolution obtained approaches the electronic noise. In grid triggering mode for the measurement of high energy $\gamma$ rays, the system is currently limited to an energy threshold above 100 keV. After the voxel-based nonuniformity correction, a FWHM of 1.75% (11.6 keV) at 662 keV was obtained for all single-pixel events in detector #1.

Several ongoing improvements in the DAQ system should yield better performance with these CZT detectors. First, by applying AC or AC equivalent coupling between VA1 chip and the detector, the equivalent electronic noise of the VA1 chip can be reduced under 4 keV according to experiment. Second, by using peak hold circuits instead of the current Sample/Hold circuits on the VA1 chip, the amplitude sampling error due to the Sample/Hold control signal can be eliminated. This is especially important for multiple-pixel events. Third, by introducing self-triggering circuits into the multi-channel readout chip, the system trigger signal can be consistently generated from the pixel signals over the full dynamic range. This will enable the energy threshold to be reduced to several keV for the measurement of high energy gamma rays. Finally, for multiple-pixel events, the timing information in the self-triggering signals can be obtained and used to reconstruct the locations of the multiple interactions in the detector. This improvement would make it possible to produce accurate nonuniformity corrections for multiple-pixel events. With the above improvements, we expect a more compact DAQ system and better energy resolution in the spectra from both single-pixel and multiple-pixel events.

## V. Acknowledgments

This work was supported under DOE Grant DOE-FG08-98NV13357. We thank F. Schopper of Max-Plank-Institute for help in the application of the hybrid board and repeater card.

## VI. References

[1] Z. He, et al., "3-D Position Sensitive CdZnTe Gamma-Ray Spectrometers", Nucl. Instr. & Meth. in Phys. Res., A 422(1999)173-178.

[2] IDE AS, Veritasveien 9, N-1322 Hovik, Norway.

[3] Amptek Inc., 6 De Angelo Drive, Bedford, MA 01730, USA.

[4] Z. He, et al., "1-D Position Sensitive Single Carrier Semiconductor Detectors", Nucl. Instr. & Meth. in Phys. Res., A 380(1996)228-231.

[5] Z. He, et al., "Effects of Charge Sharing in 3-D Position Sensitive CdZnTe Gamma-Ray Spectrometers", *the 8th European Symposium on Semiconductor Detectors*, Schloss Elmau, Germany, 1998.

[6] Y. Du, et al., "Monte Carlo Investigation of the Charge Sharing Effects in 3-D Position Sensitive CdZnTe Gamma Ray Spectrometers", *IEEE Nuclear Science Symposium*, Toronto, Canada, 1998.

[7] Z. He, et al., "Measurement of Material Uniformity using 3-D Position Sensitive CdZnTe Gamma-Ray Spectrometers", to appear in Nucl. Instr. & Meth. in Phys. Res. A.

[8] W. Li, et al., "Spatial Variation of Energy Resolution in 3-D Position Sensitive CZT Gamma-Ray Spectrometers", IEEE Trans. Nucl. Sci., Vol.46, No.3, pp. 187-192, 1999.